JMEPEG (2011) 20:679–683
DOI: 10.1007/s11665-011-9888-1

1059-9495/$19.00

Abrasive Wear of Fe-Mn-Si-Cr-Ni Shape Memory Stainless Steel: Preliminary Results

Christian Egidio da Silva, Heide Heloise Bernardi, and Jorge Otubo

(Submitted May 3, 2010; in revised form February 10, 2011)

This study was developed to understand the influence of chemical composition and austenitic grain size on the wear resistance in stainless shape memory steel. A two-body abrasive wear device was used to understand the wear mechanism involved. They were tested pins with the following chemical composition: Fe-10.3Mn-5.3Si-9.9Cr-4.9Ni-0.006C and Fe-14.2Mn-5.3Si-8.8Cr-4.6Ni-0.008C after being austenitized at 900 and 1050 °C, followed by water quenching. The surface characterization was performed by optical microscopy and scanning electron microscopy, and the roughness profile evaluation was also conducted. The weight loss was measured after conducting the wear testing, and the wear rates were estimated. The results demonstrated that the alloy with less manganese and higher chromium content has the best wear resistance (between 17.5 and 18.9%). With an increase of the austenitic grain size there was a small reduction on the wear resistance (between 3.0 and 4.1%). The chemical composition demonstrated to have higher influence on the wear behavior than the austenitic grain size.

Keywords aerospace, mechanical testing, stainless steels, surface engineering, tribology

1. Introduction

Since the 1990s, Fe-Mn-Si-based alloys such as Fe-Mn-Si-Cr-Ni and Fe-Mn-Si-Cr-Ni-Co have been studied as a candidate to substitute Ni-Ti. The shape memory effect on Fe-Mn-Si-Cr-Ni alloys is associated to a non thermoelastic martensitic transformation $\gamma(\mathrm{CFC}) \leftrightarrow \varepsilon(\mathrm{HC})$. Due to its lower shape memory effect compared to Ni-Ti, the Fe-Mn-Si-based alloys are not employed in large-scale, however, they have many potential applications. A good shape memory effect would allow expanding their industrial application (Ref 1-3). The use of Fe-Mn-Si-based alloys is justified by their lower manufacturing cost. In recent years, Fe-Mn-Si-based shape memory alloys have received much attention due to the possibility of using them in applications such as pipe joints, bolts, reinforcement of plasters, electrical actuators, thermal actuators, and vibration damping (Ref 4, 5). Ferrous SMAs based on Fe-Mn alloy system may become a new class of SMAs of great technical importance.

Works have been done by this group since 1994 (Ref 6-13) to understand the physical metallurgy involved in this material, and to optimize its shape memory recovery capacity. These works have demonstrated that besides the chemical composition, the grain size plays an important role on the shape recovery performance: the smaller the grain size the higher the shape recovery performance.

Earlier works (Ref 10-13) have revealed that no grain growth is noticed up to 900 °C of austenitizing temperature, which suggests that the energy to promote the grain growth was not enough. An abrupt grain size increase can be observed for samples austenitized in temperatures between 950 and 1050 °C. Alloys with less manganese and more chromium content are quite stable and there is no grain growth noticed up to 1000 °C. It was also observed an increase of almost two times on the grain growth when compared to the ones from austenitizing temperatures of 900 and 1050 °C.

According to Stachowiak and Batchelor (Ref 14), wear by abrasion is one form of wear caused by contact between particles and solid material. Considering that in several applications there is a mechanical contact among pieces, it is necessary to start studying wear resistance on shape memory alloy.

There are no published articles studying wear mechanism on shape memory Fe-Mn-Si-Cr-Ni stainless steel. This article presents preliminary results about the influence of chemical composition and austenitic grain size on wear resistance.

2. Experimental Procedure

Ingots (65×65 mm^2) were prepared by vacuum induction melting and their chemical composition are shown in Table 1. The ingots were heated to 1180 °C and hot forged down to 40×40 mm^2 bars. These bars were solution treated at 1100 °C for 3600 s, then hot rolled to 20 mm in diameter.

This article is an invited paper selected from presentations at Shape Memory and Superelastic Technologies 2010, held May 16-20, 2010, in Pacific Grove, California, and has been expanded from the original presentation.

Christian Egidio da Silva, Heide Heloise Bernardi, and **Jorge Otubo**, Mechanical Engineering Division, Technology Department, Aeronautical Technologic Institute, São José dos Campos, SP, Brazil; and **Christian Egidio da Silva**, Product and Process Engineering, Gerdau Aços Especiais, Pindamonhangaba, SP, Brasil. Contact e-mails: christianegidio@gmail.com and christian.silva@gerdau.com.br.

The bars were submitted to a sequence of hot swaging followed by cold forging down to 8 mm of final diameter, according to the following procedure: the 20 mm bars were initially heated to 1050 °C per 2400 s, and then hot swaged with intermediary annealing at 1050 °C, every swaging pass down to 9.5 mm in diameter; after that, these bars were cold forged down to a final diameter of 7.6 mm. After reaching the final diameter, the bars were austenitized at 900 and 1050 °C for 2400 s.

After concluding the heat treatment the bars were cut in ∅ 7.6 mm × 12 mm pins to perform wear testing. A two-body abrasive wear testing was used to assess the wear resistance, according to the following parameters: room temperature (24-28 °C), static pin, #320 grit (sandpaper) as abrasive surface, dry test (without cooling fluid), normal weight constant, 300 rpm speed and different running times (120, 240, 360, and 600 s). Before conducting the wear testing the pins were mechanically grinded (#320 to #600), and mechanically polished with diamond paste (6, 1, and ¼ μm). The same procedure was used on all the samples.

The microstructures were analyzed by SEM (JEOL JSM-6490LV) and optical microscopy (LEICA LMDM). The surface was analyzed using optical microscopy tools. The wear rate was estimated using a balance METTLER H35AR (±0.0001 g) after concluding each running time cycle on the two-body abrasive wear device. The abrasive surface (#320 grit) was changed after concluding each running cycle to avoid contamination.

Table 1 Chemical composition (wt.%)

	1	2
Cr	9.9	8.8
Ni	4.9	4.6
Mn	10.3	14.2
Si	5.3	5.3
C	0.006	0.008
Fe	Balance	Balance

3. Results and Discussion

3.1 Microstructure

Figure 1 and 2 shows the microstructures of samples before the wear testing. It is possible to notice a heterogeneous microstructure for both alloys as well as the presence of twins inside the grain distributed along its area. The difference on the grain size is visible from 900 to 1050 °C of austenitizing temperature.

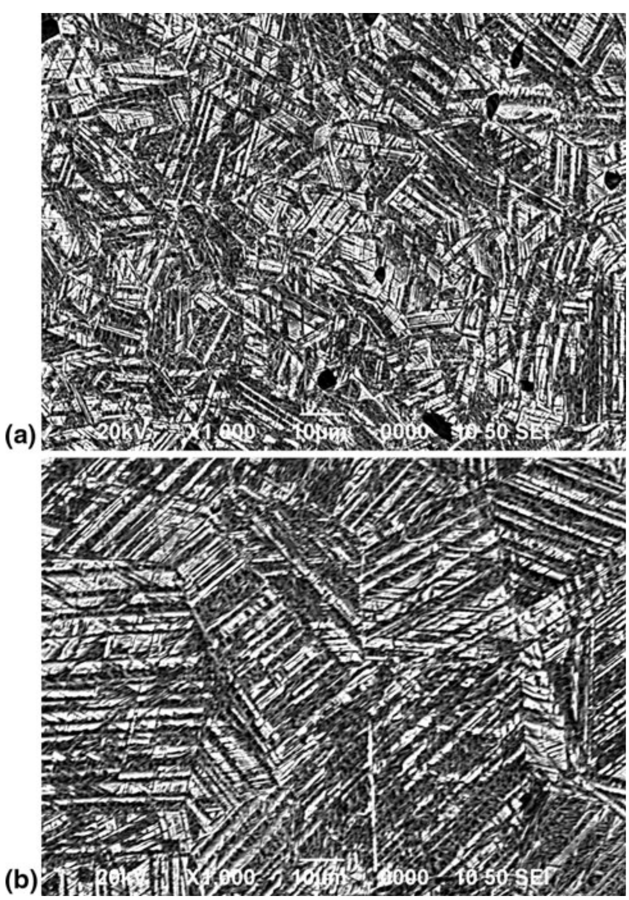

Fig. 1 Microstructures of alloy 1 at 900 °C (a) and 1050 °C (b) before testing. SEM. Etching: marble

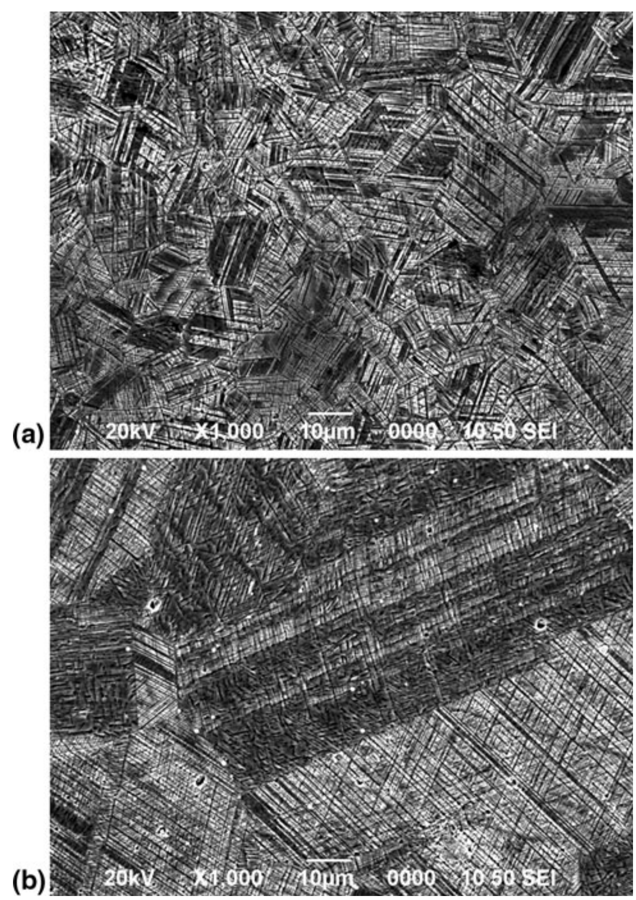

Fig. 2 Microstructures of alloy 2 at 900 °C (a) and 1050 °C (b) before testing. SEM. Etching: marble

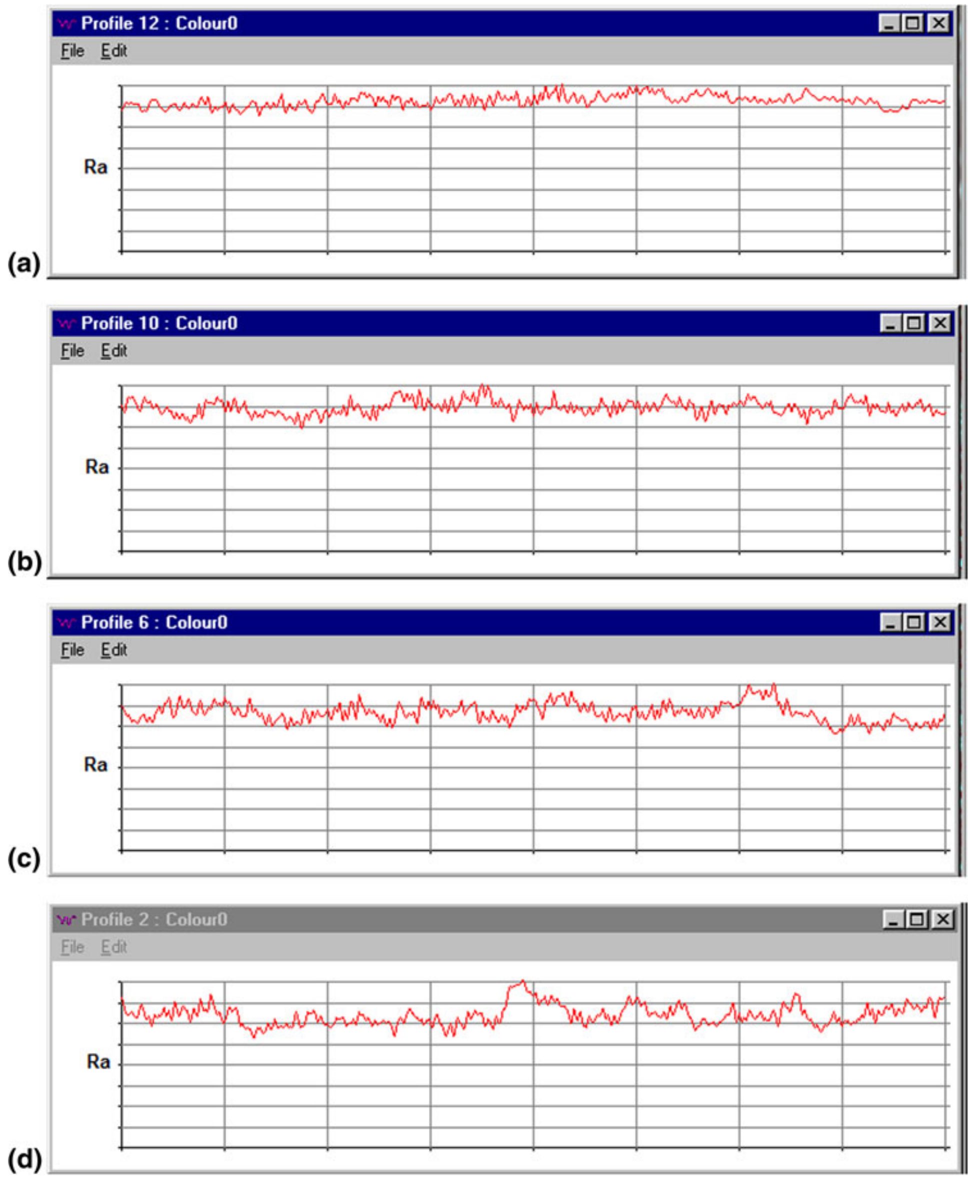

Fig. 3 Roughness profile before testing: (a) Alloy 1 at 900 °C; (b) Alloy 1 at 1050 °C; (c) Alloy 2 at 900 °C; (d) Alloy 2 at 1050 °C. Optical microscopy. Etching: marble

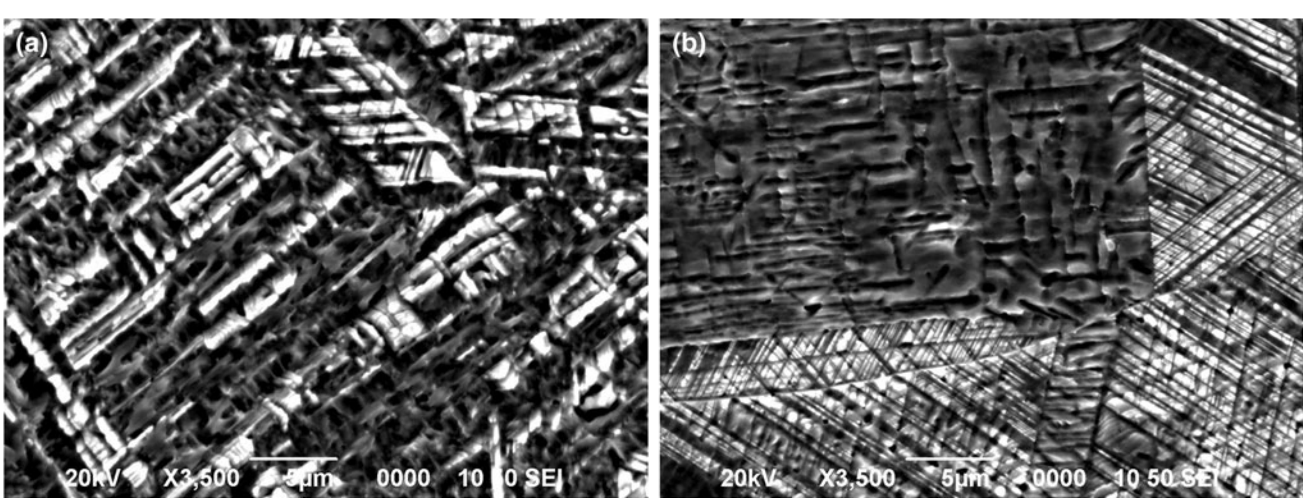

Fig. 4 Typical micrographs of alloy 1 (a) and 2 (b) after austenitizing at 1050 °C. SEM. Etching: marble

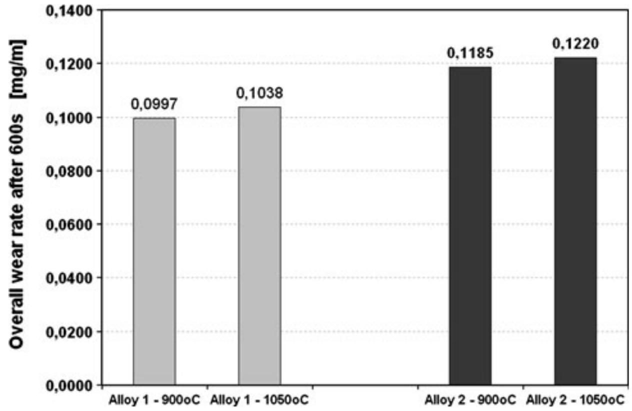

Fig. 5 Overall wear rate for both materials at different austenitizing temperatures

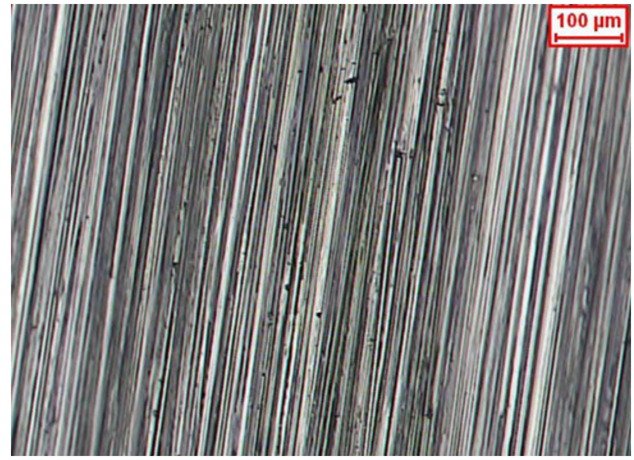

Fig. 6 Image of tracks on the surface after the contact with the abrasive

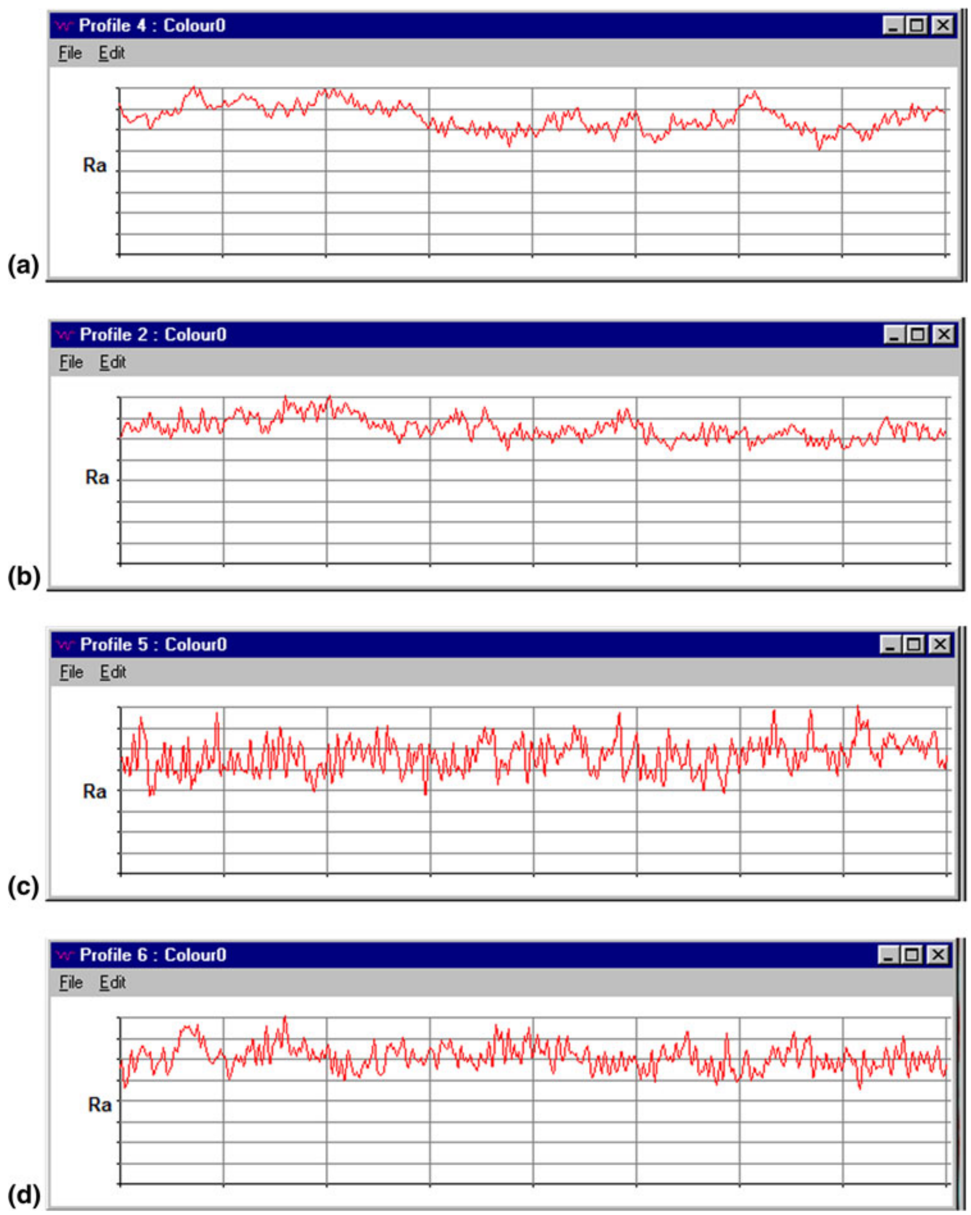

Fig. 7 Roughness profile after testing: (a) Alloy 1 at 900 °C; (b) Alloy 1 at 1050 °C; (c) Alloy 2 at 900 °C; (d) Alloy 2 at 1050 °C. Optical microscopy

3.2 Surface Characterization Before Wear Testing

Figure 3 shows the roughness profile of samples obtained by optical microscopy. It is possible to see that alloy 1 presented a more continuous roughness profile along the scanning length (less dispersive) than alloy 2.

Figure 3 suggests that an increase of the austenitizing temperature leads to an increase of roughness profile. This effect on roughness can be explained by the difference of austenitic grain size: the larger the grain size, the bigger the difference on the surface because of its structure.

Figure 4 shows typical micrographs for both materials after austenitizing at 1050 °C. This figures help to understand the difference on roughness profile of samples "1" and "2." It is noticed the existence of twins in both materials. Alloy 1 (Fig. 4a) is more homogeneously distributed than alloy 2 (Fig. 4b).

3.3 Wear Resistance

Figure 5 shows the overall wear rate for both materials after 600 s of running time. Alloy 1 showed better wear resistance than alloy 2: from 17.5% (0.1038 mg/m against 0.1220 mg/m, at 1050 °C) to 18.9% (0.0997 mg/m against 0.1185 mg/m, at 900 °C).

An increase of austenitizing temperature promoted a decrease of the wear resistance. The temperature of 900 C showed better wear resistance than of 1050 °C: from 3.0% (0.1038 mg/m against 0.0997 mg/m, for alloy 1) to 4.1% (0.1220 mg/m against 0.1185 mg/m, for alloy 2).

It is possible to infer that chemical composition has much more influence on the wear behavior than austenitic grain sizes (promoted by austenitizing heat treatment).

Figure 6 shows typical tracks on the surface of samples after wear testing. Similar tracks were noticed on both materials, and at different austenitizing temperatures. It is possible to observe (in close detail) many particles displacement along the tracks.

Figure 7 shows the roughness profile of the samples obtained by optical microscopy after wear testing. Alloy 1 presented a more continuous roughness profile along the scanning length (less dispersive) than alloy 2. This behavior can be explained by the difference in the microstructure (see Fig. 3). Alloy 2 presented a larger austenitic grain size. This causes the appearance of many more crystallographic structures for alloy 2 than alloy 1, which promotes the difference on roughness.

4. Conclusion

Both Fe-Mn-Si-Cr-Ni shape memory stainless steel presented a predominant abrasive wear micro-cutting mechanism. The material is removed as wear debris.

The alloy with less manganese and higher chromium content showed better wear resistance.

An increase of grain size resulted on a decrease of wear resistance. The larger the austenitic grain size, the rougher the profile.

Chemical composition exhibits much more influence on wear resistance than austenitic grain sizes.

References

1. S. Kajiwara, Characteristic Features of Shape Memory Effect and Related Transformation Behavior in Fe-Based Alloys, *Mater. Sci. Eng.*, 1999, **A273–275**, p 67–88
2. Y.H. Wen, M. Yan, and N. Li, Remarkable Improvement of Shape Memory Effect in Fe-Mn-Si-Cr-Ni-C Alloy by Ageing with Deformation, *Scripta Mater.*, 2004, **50**, p 835–838
3. K.K. Jee, J.H. Han, and W.Y. Jang, Measurement of Volume Fraction of ε Martensite in Fe-Mn Based Alloys, *Mater. Sci. Eng. A*, 2004, **378**, p 319–322
4. A. Baruj and H.E. Troiani, The Effect of Pre-Rolling Fe-Mn-Si-Based Shape Memory Alloys: Mechanical Properties and Transmission Electron Microscopy Examination, *Mater. Sci. Eng. A*, 2008, **481–482**, p 574–577
5. K.K. Jee, J.H. Han, and W.Y. Jang, A Method of Pipe Joining Using Shape Memory Alloys, *Mater. Sci. Eng. A*, 2006, **438–440**, p 1110–1112
6. J. Otubo, P.R. Mei, S. Koshimizu, A.H. Shinohara, and C.K. Suzuki, Relationship Between Thermomechanical Treatment, Microstructure and α' Martensite in Stainless Fe-Based Shape Memory Alloys, *Mater. Sci. Eng. A*, 1999, **273–275**, p 533–537
7. J. Otubo, F.C. Nascimento, P.R. Mei, L.P. Cardoso, and M.J. Kaufman, Influence of Austenite Grain Size on Mechanical Properties of Stainless SMA, *Mater. Trans.*, 2002, **43**(5), p 916–919
8. J. Otubo, P.R. Mei, N.B. Lima, M.M. Serna, and E. Gallego, O Efeito do Tamanho de grão Austenítico no Número de Orientações das Variantes de Martensita em Ligas Inoxidáveis com Efeito de Memória de Forma, *Rev. Escola Minas*, 2007, p 129–134 (in Portuguese)
9. F.C. Nascimento, J. Otubo, P.R. Mei, and L.P. Cardoso, Determinação das fases γ, ε e α' por difração de raios-X em ligas inoxidáveis com efeito de memória de forma, *55º Congresso Anual da ABM*, 2000 (Rio de Janeiro, RJ, Brasil), ABM, CD-ROM (in Portuguese)
10. C.E. Silva, A.R. Júnior, and J. Otubo, The Influence of Austenitizing Temperature and Chemical Composition on the Microstructure of Stainless Shape Memory Steel, *18º Congresso Brasileiro de Engenharia e Ciência dos Materiais—CBECiMat*, 2008 (Porto de Galinhas, PE, Brasil), CBECiMat, p 5875–5882
11. C.E. Silva, J. Otubo, Influência da Temperatura de Solubilização no Tamanho de Grão Austenítico de Ligas à Base de Fe-Mn-Si com Efeito de Memória de Forma: Resultados Preliminares, *63º Congresso Anual da ABM*, 2008 (Santos, SP, Brasil), ABM, p 2613–2621 (in Portuguese)
12. C.E. Silva, J. Otubo, and A.R. Júnior, A Influência do Tempo e Temperatura de Austenitização e da Composição Química na Microestrutura de Ligas Inoxidáveis com Efeito de Memória de Forma, *IX Seminário Brasileiro do Aço Inoxidável*, 2008 (São Paulo, SP, Brasil), NÚCLEO INOX, p 42–48 (in Portuguese)
13. C.E. Silva and J. Otubo, Influência da Temperatura de Austenitização na Dureza, Resistência à Compressão e Capacidade de Recuperação de Forma de Ligas Inoxidáveis, *64º Congresso Anual da ABM*, 2009 (Belo Horizonte, MG, Brasil), ABM, CD-ROM (in Portuguese)
14. G.W. Stachowiak and A.W. Batchelor, *Engineering tribology*, 3rd ed., Elsevier: Butterworth-Heinemann, Burlington, 2005, p 501–551